

# Emulating Topological Currents Arisen from Dipolar Parity Anomaly in Two-Dimensional Optical Lattices

Zhi Lin,<sup>1,2,3</sup> Xian-Jia Huang,<sup>1</sup> Dan-Wei Zhang,<sup>4,\*</sup> Shi-Liang Zhu,<sup>5,4</sup> and Z. D. Wang<sup>1,2,4,†</sup>

<sup>1</sup>*Department of Physics and Center of Theoretical and Computational Physics, The University of Hong Kong, Pokfulam Road, Hong Kong, China*

<sup>2</sup>*Shenzhen Institute of Research and Innovation, The University of Hong Kong, Shenzhen 518063, China*

<sup>3</sup>*School of Physics and Materials Science, Anhui University, Hefei 230601, China*

<sup>4</sup>*Guangdong Provincial Key Laboratory of Quantum Engineering and Quantum Materials, SPTE, South China Normal University, Guangzhou 510006, China*

<sup>5</sup>*National Laboratory of Solid State Microstructures and School of Physics, Nanjing University, Nanjing 210093, China*

We reveal topological currents arising from dipolar parity anomaly in the presence of spatiotemporally weak-dependent energy-momentum separation of paired Dirac points in two-dimensional space-time inversion symmetric semimetals. A corresponding lattice model is proposed to emulate the topological currents by using two-component ultracold atoms in a two-dimensional optical Raman lattice. In our scheme, the topological currents can be generated by varying in-site coupling between the two atomic components in time and tuned via the laser fields. Moreover, we show that the topological particle currents can directly be detected from measuring the drift of the center-of-mass of the atomic gases.

Topological states of quantum matter have been paid significant attentions in condensed matter physics [1, 2] and belong to a new classification paradigm based on the notion of topological order [3, 4], which are distinctly different from the states that are characterized by Landau theory based on spontaneous symmetry breaking [5]. In recent years, more and more interests have shifted from gapped topological insulators or superconductors to gapless topological systems, including topological semimetals with Dirac points [6–8], Weyl points [9–18], Dirac line nodes [19–25], as well as symmetry-protected  $\mathbb{Z}_2$ -type gapless points [26, 27].

On the other hand, ultracold atoms in optical lattices provide a powerful platform to simulate various quantum states of matter due to their high flexibility and controllability [28–31]. Remarkably, various topological systems have been realized and measured with ultracold atoms, such as the Hofstadter model [32, 33], Haldane model [34], two-dimensional (2D) spin-orbit-coupled systems with Dirac points [35] and with non-zero Chern numbers [36, 37], and the chiral edge states [38]. Several schemes have been proposed to realize topological semimetal bands in optical lattices [39–46]. In three-dimensional (3D) topological Weyl semimetals, there is a topological current  $\mathbf{J}_W = b_0 \mathbf{B} / 4\pi^2$  arising from the chiral magnetic effect in the presence of the energy separation of paired Weyl points  $b_0$  and the external magnetic field  $\mathbf{B}$ , which has virtually been simulated with superconducting quantum circuits in 3D parameter space [47]. Another kind of topological responses induced by axial gauge fields [48] from the energy-momentum separation between a pair of Weyl points was indicated for cold atoms in 3D optical lattices [49].

In this Letter, we reveal a distinct kind of topological currents in 2D  $\mathbb{Z}_2$ -type semimetals possessing a joint space-time inversion ( $PT$ ) symmetry [27], which is induced by the spatiotemporally dependent energy-momentum separation of paired Dirac points. We also propose a tunable lattice model, which is theoretically able to generate pure topological currents and is realizable by using two-component ultracold atoms in a 2D optical Raman lattice. In the proposed optical lattice system, the topological currents can experimentally be generated by varying in-site coupling between the two atomic components in time and tuned via the applied laser fields. Furthermore, we show that the topological particle currents can directly be detected from measuring the drift of the center-of-mass of the atomic gas.

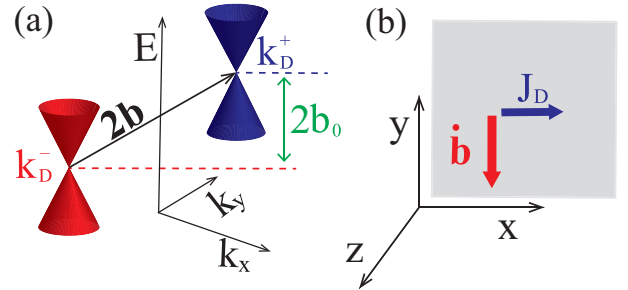


FIG. 1: (a) A sketch of the dipole momentum  $b_\mu = (b_0, \mathbf{b})$  of paired Dirac points in energy-momentum space for  $b_1 = 0$ , where  $b_\mu$  is a function of space and time. The Dirac points  $\mathbf{k}_D^+$  and  $\mathbf{k}_D^-$  are respectively in blue and red Dirac cones, with  $\pm$  denoting the two opposite parity signs. (b) A sketch of the topological current induced by the dipolar parity anomaly  $\mathbf{J}_D$  from a weak time-dependent  $\mathbf{b}$  perturbation.

*Topological currents in 2D Dirac semimetals.* We consider a 2D topological semimetal system with a single pair of Dirac points  $\mathbf{k}_D^\pm$ , as shown in Fig. 1(a). The low-energy graphene-like effective Hamiltonian of the sys-

\*Electronic address: danweizhang@m.scnu.edu.cn

†Electronic address: zwang@hku.hk

tem reads  $\mathcal{H}_{\text{eff}} = k_\mu \gamma^\mu - b_\mu \gamma^\mu \tau_z$  with  $\mu = 0, 1, 2$ , where  $\gamma^\mu$ 's are the Gamma matrices defined here in the (2+1)-dimension of space-time as  $\gamma^0 = \sigma_0 \tau_0$ ,  $\gamma^1 = \sigma_1 \tau_0$ , and  $\gamma^2 = \sigma_2 \tau_z$ , with  $\sigma_\mu$ 's being the Pauli matrices acting on the (pseudo-)spin states at each Dirac cone while  $\tau_0$  and  $\tau_z$  belonging to the other set of Pauli matrices acting on the two cones. The dipole momentum  $b_\mu$  denotes the separation of paired Dirac points in the energy-momentum space. More specifically, here  $2b_0$  denotes the energy separation and one can define the vector  $\mathbf{b} = (b_1, b_2) = (\mathbf{k}_D^+ - \mathbf{k}_D^-)/2$  denoting the momentum separation, with an example shown in Fig. 1(a). When the system is coupled with an external (effective) electromagnetic field  $A_\mu$ , the effective action gives rise to a topological term  $S_{\text{top}} = i \int d^x \epsilon^{\mu\nu\rho} b_\mu \partial_\nu A_\rho / (2\pi)$  (see a derivation in the Supplemental Material (SM) [50]). The response current of the 2D topological semimetals can be obtained by taking the functional derivative of the anisotropic Chern character term  $J^\mu = \delta S_{\text{top}} / \delta A_\mu = \epsilon^{\mu\nu\rho} \partial_\nu b_\rho$ . This implies a topological current [50]

$$\mathbf{J}_D = \frac{1}{2\pi} (\nabla b_0 - \partial_t \mathbf{b}) \times \hat{e}_z, \quad (1)$$

and the corresponding particle density is  $\rho_D = (\nabla \times \mathbf{b}) \cdot \hat{e}_z / (2\pi)$ , where we have set  $\hbar = e = c = 1$  for brevity. Obviously, the topological current  $\mathbf{J}_D$  is dependent solely on dipole momentum  $b_\mu$ , which plays a similar role as the gauge field  $A_\mu \rightarrow (b_0, \mathbf{b})$ . The above current stems from a pair of  $PT$ -protected Dirac points in two dimension, which is different from that caused by the parity anomaly of a single Dirac point (see the SM [50]), and thus may be called as topological currents of dipolar parity anomaly (DPA). To our knowledge, this kind of pure topological currents have never been probed experimentally. We note that a similar topological current may also be obtained from time-dependent elastic deformations in graphene [51], but it seems to be extremely hard to probe the current experimentally. Although the topological current is derived from an effective field theory of 2D topological semimetals under external electromagnetic fields, it can be still illustrated as the particle current in neutral atom systems with the same spatiotemporally dependent Dirac dipole momentum. Notably, when there are multi-pairs of Dirac points in the 2D topological semimetal system, the total induced topological current equals to that takes the sum of currents arising from each pair of Dirac points [47].

*Model on an optical Raman lattice.* We now turn to realization of the topological particle current  $\mathbf{J}_D$  with cold atoms in a 2D optical lattice, which can be created by slowly space-varying  $b_0$  or (and) time-varying  $\mathbf{b}$ , such that the adiabatic approximation is valid for the topological features of considered bands. For simplicity but without loss of generalization, we here focus on generating  $\mathbf{J}_D$  from time-dependent  $\mathbf{b}$  in the corresponding lattice system, as shown in Fig. 1(b). To do this, we consider to realize the following Bloch Hamiltonian on the

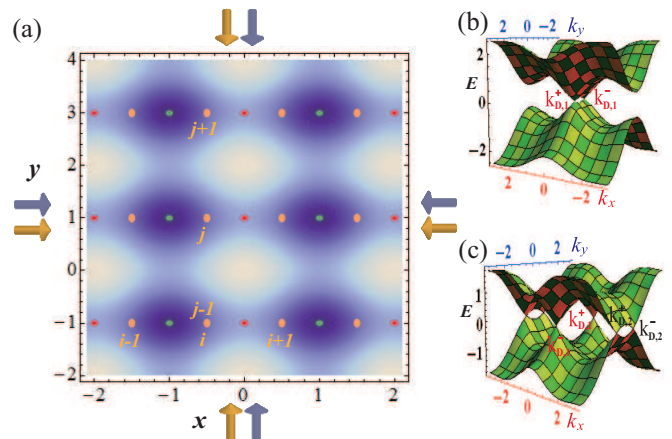


FIG. 2: (a) A sketch of Raman lattice potential  $V^R(x, y)$  as a function of  $y$  and  $x$  (in units of  $a_x$  and let  $V_{0,x}^R = V_{0,y}^R$ ). The green rings region denote the Raman lattice site (minimal Raman lattice potential  $V_{\text{Min}}^R(x, y)$ ) and the red rings denote site with potential  $V^R(x, y) = -V_{\text{Min}}^R(x, y) < V_{\text{Max}}^R(x, y)$ . Moreover, the orange ovals denote the optical lattice site  $(x_i, y_j)$ , where the  $i$  and  $j$  is the shorthand notation of  $x_i$  and  $y_j$ , respectively. The orange and light blue arrows denote the laser beams, which are used to construct the optical lattice and Raman lattice, respectively. From  $V^R(x, y)$ , we easily find  $V^R(x, y = y_j) = -V^R(x + a_x, y = y_j)$  as well as  $V^R(x, y \approx y_j) \approx -V^R(x + a_x, y \approx y_j)$  and  $V^R(x, y) = V^R(x, y + a_y)$ . Two typical topological band structures (having one or two pairs of Dirac points) are showed in (b) and (c), where the Dirac points are denoted by  $k_{D,1/2}^\pm$ , and the  $\pm$  denote the different chiralities. The parameters are  $\delta_t = 0.32$  in (b,c) and  $\lambda(\tau) = 1.2$  [ $\lambda(\tau) = 0.48$ ] in (b) [(c)], corresponding to point of blue (red) lines with  $\tau \sim 17.7$  or  $49.1$  in Fig. 3(a).

2D lattice

$$\mathcal{H}(\mathbf{k}) = \sin(k_x a_x) \sigma_1 + [\lambda(\tau) - \delta_t \cos(k_x a_x) - \cos(k_y a_y)] \sigma_2 + f(\mathbf{k}) \sigma_0, \quad (2)$$

where  $a_x$  ( $a_y$ ) is the lattice length in  $x$  ( $y$ ) direction,  $\lambda(\tau)$  denotes a time  $\tau$  dependent in-site coupling between the two atomic components,  $\delta_t$  is a hopping parameter, and  $f(\mathbf{k})$  is an arbitrary function. According to the theory of joint space-inversion ( $P$ ) and time-reversal ( $T$ ) invariant topological gapless bands [27], the Hamiltonian  $\mathcal{H}(\mathbf{k})$  supports a non-trivial class of node points with  $\mathbb{Z}_2$  topological charges. The topological stability of the system only relies on the  $PT$  symmetry with the operator  $\hat{A} = \hat{P}\hat{T} = \sigma_1 \hat{K}$ , independent of the individual  $\hat{P} = \sigma_1 \hat{I}$  and  $\hat{T} = \hat{K}\hat{I}$  here, with  $\hat{I}$  inverting the wave vector  $k$  to  $-k$  and  $\hat{K}$  the complex conjugate operator. For  $\mathcal{H}(\mathbf{k})$ , it is obvious that the individual  $P$  and  $T$  symmetries are broken, but the joint  $PT$  symmetry is preserved. We here wish to pinpoint that the topological current arisen from any dipole of Dirac points in this lattice Hamiltonian system takes the same formula as that for another dipole (i.e., Eq.(1)) derived from the afore-mentioned continuum model  $\mathcal{H}_{\text{eff}}$  because of the topological equivalence between the two dipoles.

The real-space Hamiltonian  $H$  corresponding to the Bloch Hamiltonian  $\mathcal{H}(\mathbf{k})$  is found to be

$$\begin{aligned}
H = & \frac{i}{2} \sum_j \left[ \hat{a}_{j+e_x,\uparrow}^\dagger \hat{a}_{j,\downarrow} + \hat{a}_{j+e_x,\downarrow}^\dagger \hat{a}_{j,\uparrow} \right] \\
& + i \frac{\delta_t}{2} \sum_j \left[ \hat{a}_{j+e_x,\uparrow}^\dagger \hat{a}_{j,\downarrow} - \hat{a}_{j+e_x,\downarrow}^\dagger \hat{a}_{j,\uparrow} \right] \\
& + \frac{i}{2} \sum_j \left[ \hat{a}_{j+e_y,\uparrow}^\dagger \hat{a}_{j,\downarrow} - \hat{a}_{j+e_y,\downarrow}^\dagger \hat{a}_{j,\uparrow} \right] \\
& - i\lambda(\tau) \sum_j \hat{a}_{j,\uparrow}^\dagger \hat{a}_{j,\downarrow} + \sum_{j,\sigma,\eta} t_\sigma \hat{a}_{j+\eta,\sigma}^\dagger \hat{a}_{j,\sigma} + \text{H.c.}, \quad (3)
\end{aligned}$$

where  $\boldsymbol{\eta} = (e_x, e_y)$  and  $\sigma = \uparrow, \downarrow$ . A challenge for realizing this Hamiltonian with neutral atoms is to implement the spin-flip hopping, which acts as the effective 2D spin-orbit coupling. In general, the required spin-flip hopping terms may be achieved in a 2D optical Raman lattice [36]. Particularly, they can be formed by simultaneously applying two pairs of light beams via two-photon Raman coupling with the lattice potential  $V^L(x, y)$  and Raman potential  $V^R(x, y)$ . A similar Raman lattice scheme was proposed [36] and realized in the experiment [37]. For our lattice model, we choose  $V^R(x, y) = i \{V_{0,x}^R \cos(\pi x/a_x) + V_{0,y}^R [\cos(2\pi y/a_y) + 1]\}$  and  $V^L(x, y) = V_{0,x}^L \cos^2(\pi x/a_x) + V_{0,y}^L \cos^2(\pi y/a_y)$ . The sketch of the Raman potential shown in Fig. 2(a) with  $a_y = 2a_x$ . In addition, the in-site coupling between two atomic components  $\lambda(\tau)$  in Eq. (3) can be achieved and tuned by one-photon Raman coupling (via radio-frequency or microwave fields) with the time-dependent Rabi frequency [52]. For the optical Raman lattice under tight-binding approximation, the system can be effectively described by the Hamiltonian  $H$  in Eq. (3) [50].

*Tunable topological currents.* The pairs of the Dirac points are dependent on the value of  $\lambda(\tau)$  [50]. If  $\lambda(\tau) > 1 + \delta_t$  or  $\lambda(\tau) < -(1 + \delta_t)$ , the energy band is gapped without Dirac points and thus  $\mathbf{J}_D = 0$ . If  $-(1 - \delta_t) < \lambda(\tau) < 1 - \delta_t$ , there are two pairs of Dirac points which are denoted as  $k_{D,1}^\pm = (0, \pm k_{y,1})$  and  $k_{D,2}^\pm = (\pi, \mp k_{y,2})$ , where  $k_{y,1} = \arccos[\lambda(\tau) - \delta_t]/a_y$  and  $k_{y,2} = \arccos[\lambda(\tau) + \delta_t]/a_y$ , respectively. The corresponding dipole momenta are denoted by  $2\mathbf{b}_1 = k_{D,1}^+ - k_{D,1}^- = (0, 2k_{y,1})$ ,  $2\mathbf{b}_2 = k_{D,2}^+ - k_{D,2}^- = (0, -2k_{y,2})$ ,  $2b_{0,1} = f(k_{D,1}^+) - f(k_{D,1}^-)$ , and  $2b_{0,2} = f(k_{D,2}^+) - f(k_{D,2}^-)$ . Thus, the topological current  $\mathbf{J}_D$  in this system can be written as  $\mathbf{J}_D = \mathbf{J}_D^- + \mathbf{J}_D^+$ , where  $\mathbf{J}_D^\pm = \mp \lambda'(\tau) / \{2\pi a_y [1 - (\lambda(\tau) \pm \delta_t)^2]^{1/2}\} \hat{e}_x$ , with  $\lambda'(\tau) = \partial\lambda/\partial\tau$ . Here, we set  $b_{0,1/2} = 0$  since  $f(\mathbf{k})$  (even function) only includes the spin conservation hopping. If  $1 - \delta_t < \lambda(\tau) < 1 + \delta_t$  [ $-(1 + \delta_t) < \lambda(\tau) < -(1 - \delta_t)$ ], there are only one pair of Dirac points  $k_{D,1}^\pm$  ( $k_{D,2}^\pm$ ) and the corresponding topological current is  $\mathbf{J}_D = \mathbf{J}_D^-$  ( $\mathbf{J}_D^+$ ). Two typical band structures with one and two pairs of Dirac points are shown in Figs. 2(b) and (c), respectively. It is obvious that the number of pairs of Dirac points can be controlled by ad-

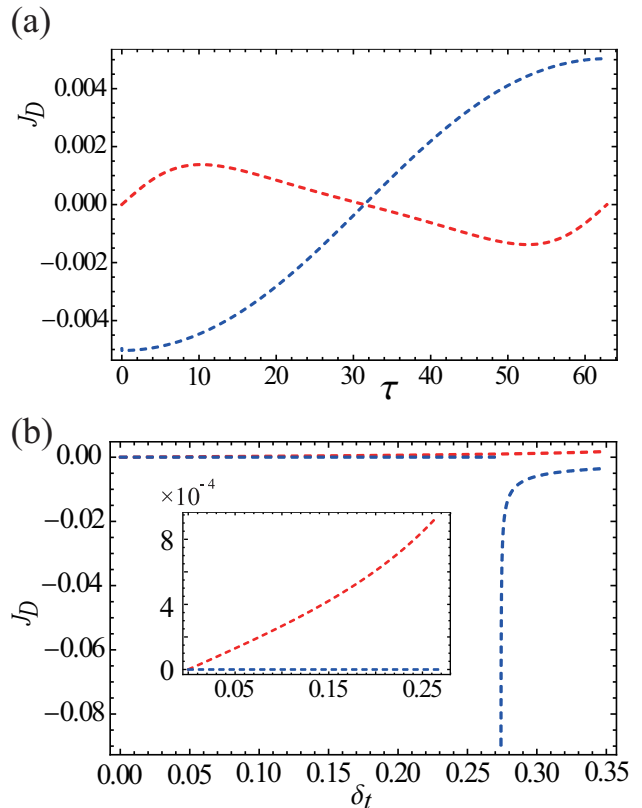


FIG. 3: The topological current  $\mathbf{J}_D$  for the slowly periodically driving case with  $\lambda = \Omega_{\text{RF}} = 0.2$  in (a) and (b) [in units of  $(a_y T_0)^{-1}$ ]. We set  $\omega \ll 1$  and  $\lambda(\tau) - \lambda_0/2 \ll 1$  for  $\forall \tau$ .  $\lambda_0 = 2.44, 1.0$  are for blue and red dashed lines, respectively. In (a), the red and blue lines denote  $\mathbf{J}_D$  for two pairs and a single pair of Dirac points, respectively, with  $\omega = \omega_{\text{max}} = 0.1$  and  $\delta_t = 0.32$ . In (b),  $\mathbf{J}_D$  as a function  $\delta_t$  with  $\tau = 10.0$  is shown. The red line denotes the case with two pairs of Dirac points, while the blue line represents the case undergoing a topological phase transition from the trivial state to the nontrivial state (a pair of Dirac points); the discontinuity of the topological currents  $\mathbf{J}_D$  reflects this topological phase transition. The insert is an enlarged figure of  $\mathbf{J}_D$ .

justing the values of  $\lambda(\tau)$  and  $\delta_t$ .

For generating tunable topological currents in the cold atom system, we also consider a typical driving forms of  $\lambda(\tau)$ : the time-periodically driving  $\lambda(\tau) = \lambda_P(\tau) = \lambda \cos(\omega\tau)/2 + \lambda_0/2$  with frequency  $\omega$ . Importantly, the time-dependent term must change slowly enough to avoid breaking the band structure. One can set the relation  $\lambda/2 |(\cos(\omega\tau + \omega T_0) - \cos(\omega\tau))| \ll t$  with  $T_0 = \hbar/t$  being satisfied, such that  $\lambda_P(\tau)$  can be considered as a quantity which changes slowly in time. Here  $\omega T_0 = \hbar\omega/t \ll 1$  is required to avoid resonance absorption for the atom-laser coupling field. Without loss of generality, we can set  $\omega_{\text{max}} T_0 = 0.1$  and  $\lambda_{\text{max}} = 0.2t$ , such that  $|(\cos(\omega\tau + \omega T_0) - \cos(\omega\tau))| \leq 0.1$  and  $|\lambda(\tau + T_0) - \lambda(\tau)|_{\text{max}} = 0.01t \ll t$ . For the time-periodically driving case, the parameters  $\lambda$ ,  $\omega$  and  $\tau$  are the compact notations of  $\lambda/t$ ,  $\omega T_0$  and  $\tau/T_0$ , respectively, which are used

to calculate  $\mathbf{J}_D$ . In this notation,  $\mathbf{J}_D$  takes the unit of  $(a_y T_0)^{-1}$ . The typical topological currents  $\mathbf{J}_D$  for the periodically driving case are shown in Figs. 3 (a) and (b). For  $\lambda_P(\tau)$ , one can regulate the number of the pairs of Dirac points through driving the system. The discontinuity of the topological current  $\mathbf{J}_D$  shown in Fig. 3 (b) is due to the change of the number of paired Dirac points. This indicates the topological phase transition of the system and means that one can induce the topological phase transition by adjusting the driving parameters.

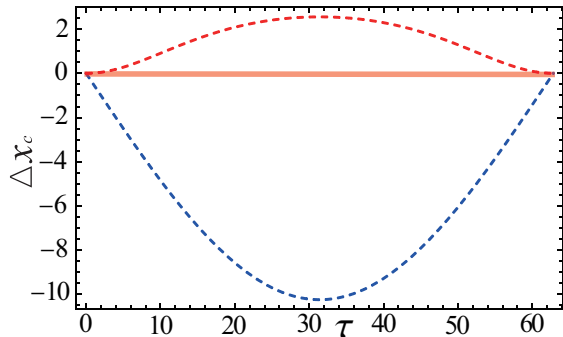


FIG. 4: The drift of the center-of-mass  $\Delta x_c = x_c(\tau) - x_c(\tau = 0)$  (in units of  $a_x$ ) as a function of  $\tau$  in  $x$  direction are shown by taking  $\rho = 0.01(a_y a_x)^{-1}$ . The parameters for blue and red dashed lines are the same as those in Fig. 3 (a). Here the parameters for the red transparent thick line are the same as the others color lines except  $\delta_t$ , where  $\delta_t$  is 0 (0.32) for the red transparent thick line (the others lines). It is clear that there is no drift of the center-of-mass  $\Delta x_c$  for  $\delta_t = 0$ , even though there are two pairs of Dirac points (due to the current cancellation from the two pairs). Thus this non-vanishing  $\Delta x_c$  feature may be taken as an experimental signature for topological currents of DPA.

*Detection schemes.* In order to observe this novel topological current in experiments, we first discuss typical energy scales for several physical quantities. For cold alkalis atoms trapped in the optical lattice, the typical recoil energy  $E_R/(\hbar \times 2\pi)$  is about several kHz [53], and the typical hopping amplitude  $t$  is changed in the region  $(0, 0.1E_R)$ . The coherence time of cold atom systems is typically around  $\tau_{\text{coh}} \sim 100\text{ms}$ . Thus, the intrinsic timescale of the lattice system is  $T_0 = \hbar/t = (1, 10, 100, 1000)\text{ms}$ , corresponding to  $t = (1000, 100, 10, 1)\text{Hz}$ . The bosonic or fermionic atoms can be loaded in the optical Raman lattice, and we assume the bosons as used in the experiment [37]. The critical temperature of typical Bose gases is about 1 – 100nK and the corresponding frequency is about 20 – 2000Hz. When the trapping potential satisfies  $V_{0,x/y}^L \gtrsim 5E_R^{x/y}$ , the atoms trapped in optical lattice are well described within the tight-binding approximation [53]. The bandwidth  $W \approx 4(t'_{0,x} + t'_{0,y} + t_x + t_y)$  is several kHz (the corresponding temperature is several hundred nK) for the 2D systems, where  $t'_{0,x/y}$  is amplitude of normal hopping.

Thus, if the temperature of system is about several hundred nK (the same level of bandwidth  $W$ ), we can assume the bosonic atoms will be incoherent homogeneous distribution within each band in  $\mathbf{k}$ -space [33] (each  $\mathbf{k}$  can be equally filled). Under these conditions, the topological current  $\mathbf{J}_D$  can be directly detected via measuring the drift of the center-of-mass of the atomic cloud along the  $x$  direction.

The measurement of the atomic center-of-mass shift can be achieved by the same way as that in the experiment in Ref. [33], but without an external effective force since the topological current arises from the time-varying fields here. The drift velocity reads  $v_c = \mathbf{J}_D/\rho$ , where  $\rho$  denotes the average density of the atomic gas and is assumed invariable within the coherence time. Thus the atomic center-of-mass displacement reads  $x_c(\tau) = \int \mathbf{J}_D d\tau/\rho$ , which directly reveals the features of  $\mathbf{J}_D$ . The typical results of the drift of the center-of-mass  $\Delta x_c = x_c(\tau) - x_c(\tau = 0)$  as a function of time  $\tau$  are shown in Fig. 4 for the periodically-driving case with  $\rho = 0.01(a_y a_x)^{-1}$  [the corresponding topological currents  $\mathbf{J}_D$  are shown in Fig. 3(a)]. In Fig. 4(a), the dashed blue lines indicate the maximum drift of  $|\Delta x_c|$ . To detect  $\mathbf{J}_D$  for the hopping amplitude  $t \sim 1\text{kHz}$ , the particle density  $\rho$  must be smaller than  $0.1(a_y a_x)^{-1}$ . This can be achieved by setting the particle number  $N \lesssim 1000$  for the typical 2D optical lattice of size  $100a_x \times 100a_y$ . If we set the density of particle  $\rho = 0.1, 0.05, 0.01(a_y a_x)^{-1}$ , the corresponding maximum displacement of  $|\Delta x_c|$  is about  $1a_x, 2a_x, 10a_x$  with  $\tau \sim 31.4\text{ms}$ , which can be well measured in cold-atom experiments [33]. Finally we note that the topological current  $\mathbf{J}_D$  is protected by the joint  $PT$  symmetry, which can also be tested in experiments. If we add  $P$  or (and)  $T$  broken perturbation term, such as  $\mathcal{H}' = \epsilon \sin(k_y a_y)$  with a small value  $\epsilon$ ,  $\mathbf{J}_D$  is not destroyed. If we add the  $PT$  symmetry broken term, such as  $\epsilon \sigma_z$  in this system, the bands will be gapped and then  $\mathbf{J}_D$  will disappear.

*Conclusion.* We have revealed a novel kind of topological currents arising from the DPA in the presence of the spatiotemporally weak-dependent energy-momentum separation of paired Dirac points in 2D  $PT$  symmetric semimetals. In particular, we have proposed an experimentally feasible scheme to realize and detect this kind of topological particle currents with ultracold atoms in a 2D optical lattice. The present scheme is quite promising for realizing the first experimental detection of topological currents of DPA.

We thank Y. X. Zhao for helpful discussions. This work was supported by the NKRD of China (Grant No. 2016YFA0301800), the NSFC (Grants No. 11604103, No. 11474153, and No. U1830111), the NSF of Guangdong Province (Grant No. 2016A030313436), the Startup Foundation of SCNU, and the GRF of Hong Kong (Grants No. HKU 173309/16P and No. HKU173057/17P).



- 
- [1] M. Z. Hasan and C. L. Kane, *Rev. Mod. Phys.* **82**, 3045 (2010).
- [2] X. L. Qi and S. C. Zhang, *Rev. Mod. Phys.* **83**, 1057 (2011).
- [3] X. G. Wen, *Adv. Phys.* **44**, 405 (1995).
- [4] D. J. Thouless, M. Kohmoto, M. P. Nightingale, and M. den Nijs, *Phys. Rev. Lett.* **49**, 405(1982).
- [5] P.W. Anderson, *Basic Notions of Condensed Matter Physics* (Westview Press, Boulder, 1997).
- [6] Z. K. Liu et al., *Nat. Mater.* **13**, 677 (2014).
- [7] M. Neupane et al., *Nat. Commun.* **5**, 4786 (2014).
- [8] S. Y. Xu et al., *Science* **347**, 294 (2015).
- [9] X. Wan, A. M. Turner, A. Vishwanath, and S. Y. Savrasov, *Phys. Rev. B* **83**, 205101 (2011).
- [10] P. Hosur and X. Qi, *C.R. Phys.* **14**, 857 (2013).
- [11] O. Vafek and A. Vishwanath, *Annu. Rev. Condens. Matter Phys.* **5**, 83 (2014).
- [12] S. Y. Xu et al., *Science* **349**, 613 (2015).
- [13] B. Q. Lv et al., *Phys. Rev. X* **5**, 031013 (2015).
- [14] S. Y. Xu et al., *Nat. Phys.* **11**, 748 (2015).
- [15] L. S. Xie, L. M. Schoop, E. M. Seibel, Q. D. Gibson, W. Xie, and R. J. Cava, *APL Mater.* **3**, 083602 (2015).
- [16] M. N. Ali, Q. D. Gibson, T. Klimczuk, and R. J. Cava, *Phys. Rev. B* **89**, 020505 (2014).
- [17] G. Bian et al., *Nat. Commun.* **7**, 10556 (2016).
- [18] L. M. Schoop, M. N. Ali, C. Straßer, V. Duppl, S. S. P. Parkin, B. V. Lotsch, and C. R. Ast, *Nat. Commun.* **7**, 11696 (2016).
- [19] C. Fang, Y. Chen, H.-Y. Kee, and L. Fu, *Phys. Rev. B* **92**, 081201 (2015).
- [20] C. K. Chiu and A. P. Schnyder, *J. Phys. Conf. Ser.* **603**, 012002 (2015).
- [21] Y. H. Chan, C. K. Chiu, M. Y. Chou, and A. P. Schnyder, *Phys. Rev. B* **93**, 205132 (2016).
- [22] Y. Kim, B. J. Wieder, C. L. Kane, and A. M. Rappe, *Phys. Rev. Lett.* **115**, 036806 (2015).
- [23] R. Yu, H. Weng, Z. Fang, X. Dai, and X. Hu, *Phys. Rev. Lett.* **115**, 036807 (2015).
- [24] K. Mullen, B. Uchoa, and D. T. Glatzhofer, *Phys. Rev. Lett.* **115**, 026403 (2015).
- [25] Y. Chen, Y. Xie, S. A. Yang, H. Pan, F. Zhang, M. L. Cohen, and S. Zhang, *Nano Lett.* **15**, 6974 (2015).
- [26] Y. X. Zhao and Z. D. Wang, *Phys. Rev. Lett.* **110**, 240404 (2013); *ibid* **116**, 016401.
- [27] Y. X. Zhao, A. P. Schnyder, and Z. D. Wang, *Phys. Rev. Lett.* **116**, 156402 (2016).
- [28] M. Lewenstein, A. Sanpera, V. Ahufinger, B. Damski, A. S. De, and U. Sen, *Adv. Phys.* **56**, 243 (2007).
- [29] I. Bloch, J. Dalibard and S. Nascimbène, *Nat. Phys.* **8**, 267 (2012).
- [30] I. Bloch, J. Dalibard, and W. Zwerger, *Rev. Mod. Phys.* **80**, 885 (2008).
- [31] J. Dalibard, F. Gerbier, G. Juzeliūnas, and P. Öhberg, *Rev. Mod. Phys.* **83**, 1523 (2011); N. Goldman, G. Juzeliūnas, P. Öhberg, and I. B. Spielman, *Rep. Prog. Phys.* **77**, 126401 (2014).
- [32] M. Aidelsburger, M. Atala, M. Lohse, J. T. Barreiro, B. Paredes, and I. Bloch, *Phys. Rev. Lett.* **111**, 185301 (2013); H. Miyake, G. A. Siviloglou, C. J. Kennedy, W. C. Burton, and W. Ketterle, *Phys. Rev. Lett.* **111**, 185302 (2013).
- [33] M. Aidelsburger, M. Lohse, C. Schweizer, M. Atala, J. T. Barreiro, S. Nascimbene, N. R. Cooper, I. Bloch, and N. Goldman, *Nat. Phys.* **11**, 162 (2015).
- [34] G. Jotzu, M. Messer, R. Desbuquois, M. Lebrat, T. Uehlinger, D. Greif, and T. Esslinger, *Nature* **515**, 237 (2014).
- [35] L. Huang, Z. Meng, P. Wang, P. Peng, S.-L. Zhang, L. Chen, D. Li, Q. Zhou, and J. Zhang, *Nat. Phys.* **12**, 540 (2016); Z. Meng, L. Huang, P. Peng, D. Li, L. Chen, Y. Xu, C. Zhang, P. Wang, and J. Zhang, *Phys. Rev. Lett.* **117**, 235304 (2016).
- [36] X.-J. Liu, K. T. Law and T. K. Ng, *Phys. Rev. Lett.* **112**, 086401 (2014).
- [37] Z. Wu, L. Zhang, W. Sun, X.-T. Xu, B.-Z. Wang, J.-C. Ji, Y. Deng, S. Chen, X.-J. Liu, and J.-W. Pan, *Science* **354**, 83 (2016).
- [38] M. Mancini et al., *Science* **349**, 1510 (2015); B. K. Stuhl, H. I. Lu, L. M. Aycocck, D. Genkina, and I. B. Spielman, *Science* **349**, 1514 (2015).
- [39] J. H. Jiang, *Phys. Rev. A* **85**, 033640 (2012).
- [40] T. Dubcek, C. J. Kennedy, L. Lu, W. Ketterle, M. Soljacic and H. Buljan, *Phys. Rev. Lett.* **114**, 225301 (2015).
- [41] D.-W. Zhang, S.-L. Zhu, and Z. D. Wang, *Phys. Rev. A* **92**, 013632 (2015).
- [42] W.-Y. He, S. Zhang, and K. T. Law, *Phys. Rev. A* **94**, 013606 (2016).
- [43] Y. Xu and L.-M. Duan, *Phys. Rev. A* **94**, 053619 (2016).
- [44] D.-W. Zhang, Y. X. Zhao, R.-B. Liu, Z.-Y. Xue, S.-L. Zhu, and Z. D. Wang, *Phys. Rev. A* **93**, 043617 (2016).
- [45] Y.-Q. Zhu, D.-W. Zhang, H. Yan, D.-Y. Xing, S.-L. Zhu, *Phys. Rev. A* **96**, 033634 (2017).
- [46] H. Hu, J. Hou, F. Zhang, and C. Zhang, *Phys. Rev. Lett.* **120**, 240401 (2018).
- [47] X. S. Tan, Y. X. Zhao, Q. Liu, G. M. Xue, H. F. Yu, Z. D. Wang, Y. Yu, arXiv: 1802.08371 (2018).
- [48] Z.-M. Huang, J. Zhou, and S.-Q. Shen, *Phys. Rev. B* **96**, 085201 (2017).
- [49] S. Roy, M. Kolodrubetz, N. Goldman and A. G. Grushin, *2D Mater.* **5**, 024001 (2018).
- [50] See the supplemental materials for more details on the derivation of topological currents arising from dipolar parity anomaly, the atomic spin-flip-hopping in the 2D optical Raman lattice, and the number of pairs of Dirac points.
- [51] A. Vaezi, N. Abedpour, R. Asgari, A. Cortijo, and María A. H. Vozmediano, *Phys. Rev. B* **88**, 125406 (2013).
- [52] P. Schauß, J. Zeiher, T. Fukuhara, S. Hild, M. Cheneau, T. Macr, T. Pohl, I. Bloch, and C. Gross, *Science* **347**, 1455 (2015).
- [53] K. Levin, A. L. Fetter, D. M. Stamper-Kurn., eds. *Ultracold Bosonic and Fermionic Gases* (Elsevier, Amsterdam, 2012).